

Automatic Brain Lesion Detection and Classification Based on Diffusion-Weighted Imaging using Adaptive Thresholding and a Rule-Based Classifier

N.M. Saad^{#1}, Syed A.R. Abu-Bakar^{*2}, A.F. Muda^{#3}, Sobri Muda^{**4}, A. R. Syafeeza^{#5}

[#] Faculty of Electronics and Computer Engineering, Universiti Teknikal Malaysia Melaka, Malaysia

¹ norhashimah@utem.edu.my, ³ m021310048@student.utem.edu.my, ⁵ syafeeza@utem.edu.my

^{*} Computer Vision, Video and Image Processing Research Lab, Faculty of Electrical Engineering, Universiti Teknologi Malaysia, Malaysia

² syed@fke.utm.my

^{**} Radiology Department, Medical Centre, Universiti Kebangsaan Malaysia, Malaysia

⁴ sobri_muda@yahoo.com

Abstract—In this paper, a brain lesion detection and classification approach using thresholding and a rule-based classifier is proposed. Four types of brain lesions based on diffusion-weighted imaging i.e. acute stroke, solid tumor, chronic stroke, and necrosis are analyzed. The analysis is divided into four stages: pre-processing, segmentation, feature extraction, and classification. In the detection and segmentation stage, the image is divided into 8x8 macro-block regions. Adaptive thresholding technique is applied to segment the lesion's region. Statistical features are measured on the region of interest. A rule-based classifier is used to classify four types of lesions. Jaccard's similarity index of the segmentation results for acute stroke, solid tumor, chronic stroke, and necrosis are 0.8, 0.55, 0.27, and 0.42, respectively. The classification accuracy is 93% for acute stroke, 73% for solid tumor, 84% for chronic stroke, and 60% for necrosis. Overall, adaptive thresholding provides high segmentation performance for hyper-intensity lesions. The best segmentation and classification performance is achieved for acute stroke. The establishment of the technique could be used to automate the diagnosis and to clearly understand major brain lesions.

Keyword- Diffusion-weighted Imaging, Brain Lesion, Adaptive Thresholding, Rule-Based Classifier

I. INTRODUCTION

Diffusion-weighted imaging (DW-MRI or DWI) is an imaging technique that provides unique information on diffusion properties of water molecules in brain tissues. It provides a contrast image that is dependent on the molecular motion of water that may be altered by diseases. DWI has been continually improved to probe the random microscopic motion of water protons on a pixel basis, as it plays a key role in evaluating multiple neurologic diseases, especially acute stroke [1-3]. It also gives additional information for cerebral diseases such as stages in neoplasm (cancers, tumors, and necrosis), infections, and others. In the United States, the estimated number of new brain cancers are increasing from 17,000 in 2009 to 23,380 in 2014, while strokes effect nearly 750,000 new cases a year [3, 4]. In July 2012, it was reported by the Ministry of Health Malaysia that brain neoplasms (tumors) and cerebrovascular diseases (strokes) are the third-and fourth-leading causes of death, respectively, in Malaysia [5].

The diagnosis of a brain lesion presents a challenging task to clinicians and neuro-radiologists because the interpretation of the clinical and imaging appearances is very subjective. It can often be difficult for clinicians to assess precisely the tissue composition of a lesion on the basis of radiographic images. Only neuro-radiologists can perform this task. Therefore, clinicians continuously seek better imaging techniques and tools to aid diagnosis. According to quantitative analysis, computer-aided diagnosis (CAD) can aid radiologists in interpreting medical images. With CAD, radiologists apply the computer output as a second opinion in making the decision [6]. As brain imaging techniques continually evolve, new and more powerful image processing techniques are required in the CAD system to meet the challenges imposed by modern medical imaging [7].

Lesion detection and segmentation are challenging tasks due to the complexity and large variations in the anatomical structures of human brain tissues. Segmentation allows for extraction of certain regions to provide further information during other stages of quantitative assessment. Accurate segmentation of the brain is the basis for calculating important information; for example, size, compactness, and volume of the lesion. Many approaches have been proposed by various researchers to deal with MRI images. The computerized method is still evolving and far from being perfect because of the system's instability in achieving autonomous property [8]. The commonly used segmentation and detection techniques can be classified into two broad categories: (1)

region-based techniques that look for the regions satisfying given homogeneity criteria and (2) edge-based segmentation techniques that look for edges in partition regions with different characteristics. Well-known and widely used brain tissue classification techniques are the unsupervised clustering algorithm and fuzzy c-means (FCM) and the supervised method such as the neural network classifier [9–11]. Novel segmentation and classification techniques should be able to overcome the limitations of the classical image-processing techniques as well as be general enough to address a large class of tissue types, thus contributing to a faster performance and higher accuracy in a fully automatic system.

Thresholding is one of the popular methods used in segmentation. Segmentation is compared based on the intensity values. Proper pre-processing analysis and selection of threshold values are vital because histogram thresholding is mainly dependent on intensity values. The main drawback of the technique is that the problem of overlapping pixel intensity in brain tissues and background cannot be resolved. Moreover, high sensitivity of homogeneity change in the soft tissue region surrounding the lesion may deteriorate the result [8]. Moreover, popular techniques such as classical region growing are semi-automated and rely heavily on the grey-level similarity, size, and connectivity that bear a risk of combining fuzzy edges around regions [12, 13].

Diffusion weighted imaging (DWI) is considered as the most sensitive technique in detecting acute infarction and is useful in giving details of the component of brain lesions [13]. In DWI, image intensity and contrast only depend on the strength of diffusivity of tissue. Tissue with altered diffusion rates may appear with either hyper- or hypo-intensity, which is absent in healthy tissue. Such information forms vital image characteristics that may lead to the classification of several brain-related diseases. For instance, acute stroke and solid tumor lesions may be seen as high intensity, while chronic stroke and necrosis appear as low intensity. Visually, there might be intensity overlapping in these lesions [14]. The result from quantitative analysis can be performed detect and classify the lesions. Therefore, our hypothesis is that it is feasible to automatically detect the hyper- and hypo-intensity lesions in DWI by using a simple adaptive thresholding method. Furthermore, a brain classification system can be developed based on the features in the DWI images.

Basic thresholding of brain lesion has been discussed in [15]. However, the proposed methodology in the previous paper was dependent on average optimal thresholding values and not adaptive. Furthermore, the number of samples used was limited to 20 samples. In this paper, we propose an adaptive thresholding technique to automatically detect and threshold the lesions in DWI. Gradient function is used to adaptively calculate the optimal thresholding values. In the feature extraction stage, several statistical ROI measurements such as mean, size, area, boundary, and compactness are measured. These features are used as input for classification. Rule-based classifier is implemented in the classification stage to classify acute stroke, solid tumor, chronic stroke and necrosis. Number of samples used are 75. This paper is organized as follows. Section 2 discusses the proposed materials and methods. The flowchart of the segmentation process is detailed. The results are discussed in section 3. Finally, section 4 concludes the paper.

II. MATERIALS AND METHODS

A. Flowchart of the Proposed System Design

Fig. 1 shows the flowchart for the whole analysis. First, the samples of the brain DWI dataset are collected. For the pre-processing stage, several algorithms are applied for normalization, background removal, and intensity enhancement. In order to extract the region of interest (ROI) of the lesion, an image segmentation algorithm is applied. The characteristics of lesions are then measured using statistical calculation. Finally, a rule-based classifier is designed to classify the type of brain lesion. The performance of the proposed methods is evaluated based on the accuracy of the system.

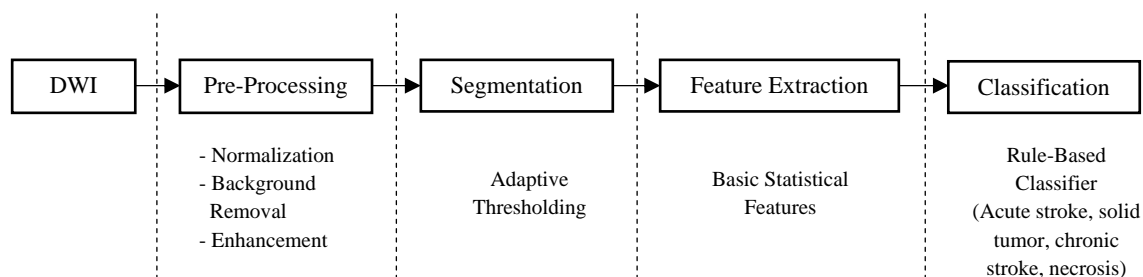


Fig. 1. Flowchart of the Proposed System Design

B. Image Dataset

The DWI images are collected from the General Hospital of Kuala Lumpur using 1.5T MRI scanners (Siemens Magnetom Avanto). The parameters obtained from this scanner are time echo (TE), 94ms; time repetition (TR), 3200ms; pixel resolutions, 256x256; slice thickness, 5mm; gap between each slice, 6.5 mm; intensity of diffusion weighting known as b value, 1000 s/mm²; and total number of slices, 19. The data is

encoded in 12-bit DICOM (Digital Imaging and Communication in Medicine) format. The dataset consists of 30 samples of acute infarctions and 15 samples of solid tumors which both represent the hyper-intensity lesions. Hypo-intensity lesions are represented by 20 samples of chronic strokes and 10 samples of necrosis. Overall, 75 images were taken for this analysis.

In the imaging dataset, diagnosis and medical report were made by the minimum of two neuro-radiologists. The report including patient symptoms on different cases, clinical history, preoperative diagnosis, clinical tumor grades or features obtained from surgery or histological tests, and imaging findings. With the aid of the experts, the features such as image intensity, image structures, lesion's shape, contour, tumor capsules, necrosis or cyst generation, any bleeding and calcifications, and other infections were study and highlighted. These images were segmented and marked manually by the specialists to show the lesion area. Fig. 2 shows the example of the images obtained for this analysis. The lesions are marked with red arrows.

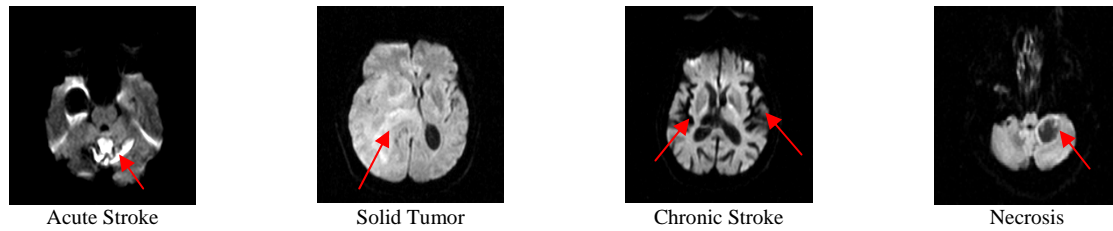
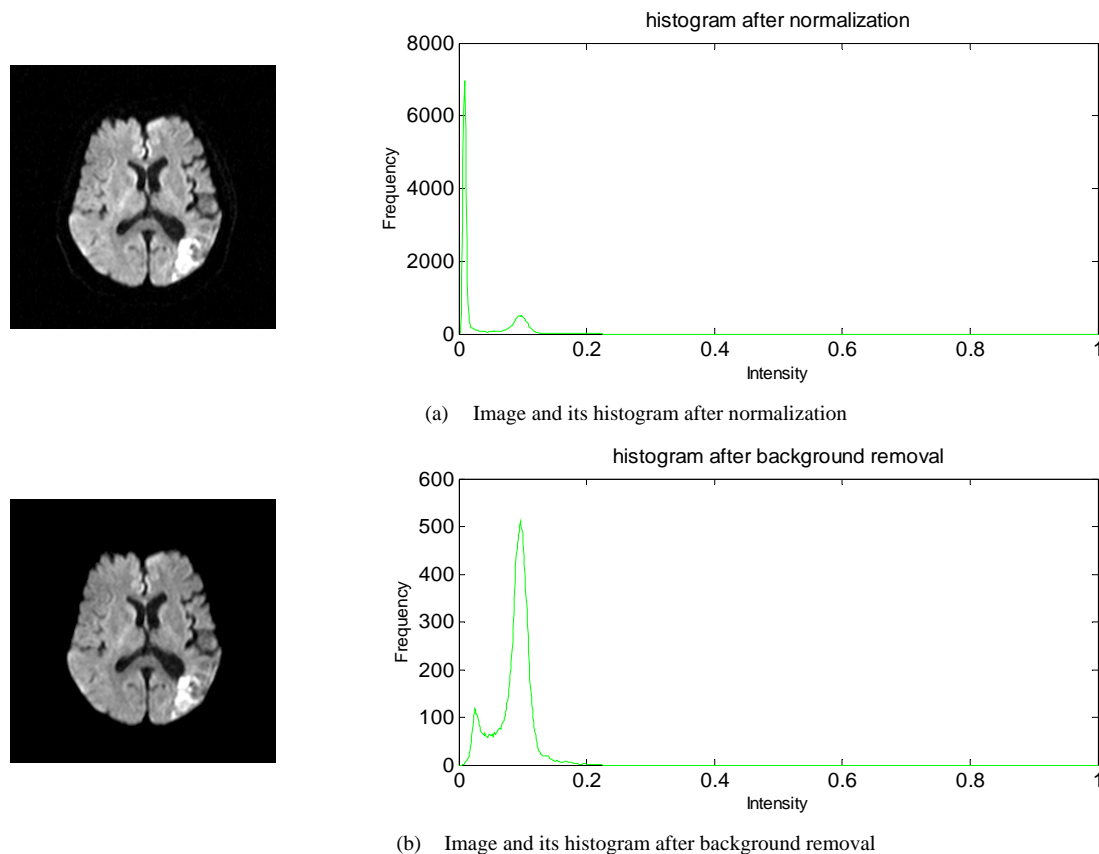
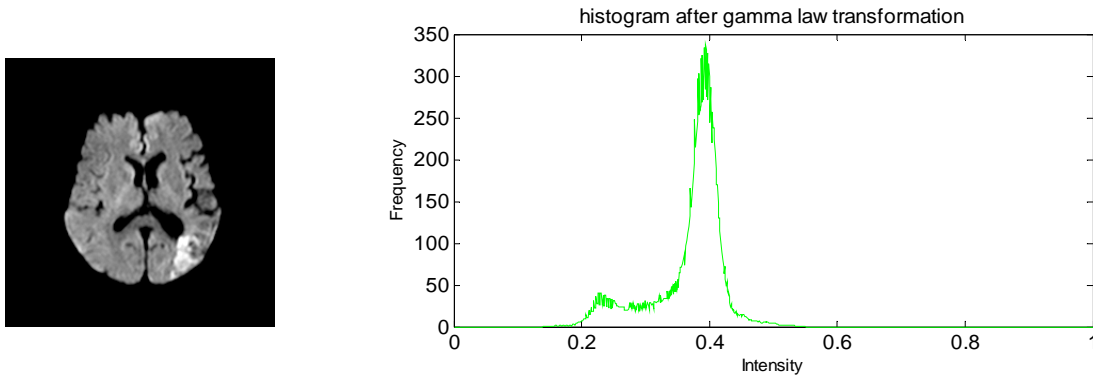


Fig. 2. Image of DWI Lesions

C. Pre-Processing Stage

Fig. 3 shows one image sample at pre-processing stage. The gray level values from 12-bit unsigned integer (0-4095) are then normalized to floating point values (0 to 1). The background needs to be removed since it has the largest number of low value pixels. This process is carried out using Otsu's method [16] before the outer brain boundary is detected. Pixels inside the brain boundary are set to "1" while the background pixels are set to "0". The brain image is then obtained by multiplying this binary image to the original image. Gamma law transformation algorithm [12] is applied to enhance the narrow range of the low-input gray level values. According to the experiment, the best value for γ , the constant power is 0.4. The original image and its histogram are shown in Fig. 3(a). Fig. 3(b) shows all the background pixels that have been removed and have produced a better shape of the image histogram. The maximum peak is at 0.1. The histogram has been expanded such that the peak is located at 0.4 after gamma law transformation is applied, as shown in Fig. 3(c).





(c) Image and its histogram after gamma law transformation

Fig. 3. Pre-Processing Stage

D. Segmentation Stage

We apply adaptive thresholding segmentation in segmenting the brain lesion. The image is first divided into 8x8 macro-block regions, where 256x256 pixels are separated to 16x16 pixels size in each region as shown in Fig. 4. The lesion's area is indicated by the red circle at (see region 46).



Fig. 4. 16x16 Pixels per Macro-block Region

Fig. 5 shows the histogram that has been calculated at each region. The red circle shows the corresponding histogram of lesion in region 46, whereas other regions are normal. All regions are superimposed to find the maximum number of pixels at each intensity level.

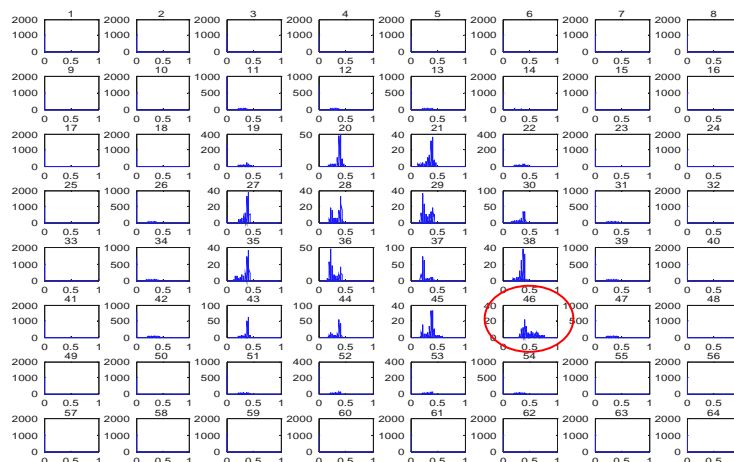


Fig. 5. Histogram Distribution of Each Region

The maximum number of pixels is calculated by using the function shown in Equation (1), as follows.

$$P_{\max}(i) = \text{Max}(P(R_1 : R_m, i)) \tag{1}$$

where $P(i)$ is the intensity at level i , and R_1 to R_m are the number of pixels in i^{th} macro-block region. This will produce a new histogram as shown in Fig. 6.

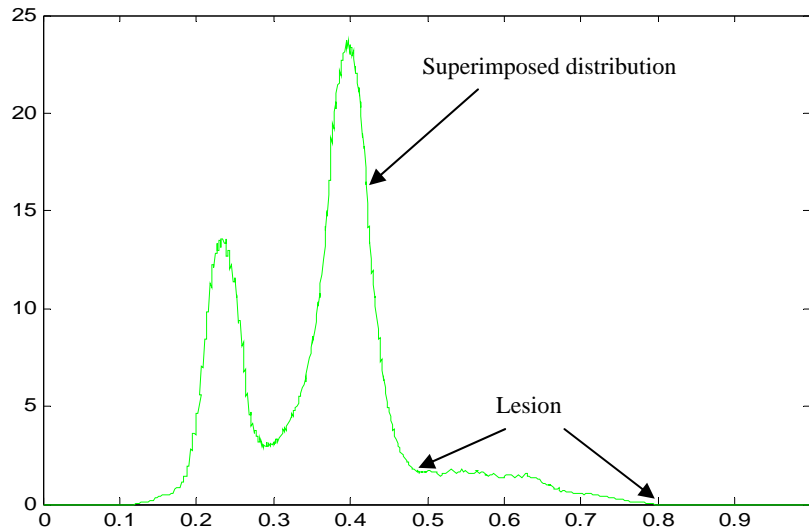


Fig. 6. Superimposed Histogram

Gradient function (Equation 2) is used to adaptively calculate the minimum and maximum thresholding values. The gradient values reach maximum when the histogram has the greatest rate of change, and vice versa. The minimum and maximum thresholds (T_1 and T_2) are set at the first zero-gradient before and after the maximum peak, respectively. This histogram is shown in Fig. 7.

$$\text{div}(i) = \frac{dy}{dx} P(i) \tag{2}$$

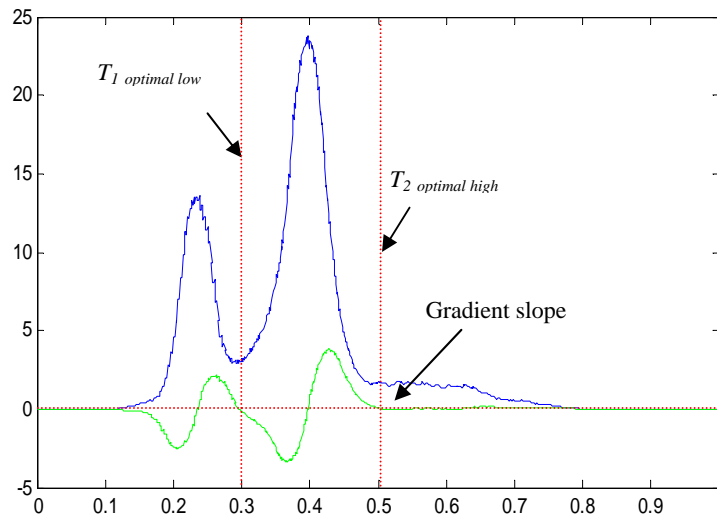


Fig. 7. Gradient Slope to Determine the Optimal Threshold

The two regions of hyper- and hypo-intense are then calculated according to Equations (3) and (4).

$$I(x, y)_{\text{hypo-intense}} = \begin{cases} 1 & \text{for } I(x, y) \leq T_{1\text{low}} \\ 0 & \text{elsewhere} \end{cases} \tag{3}$$

$$I(x, y)_{\text{hyper-intense}} = \begin{cases} 1 & \text{for } I(x, y) \geq T_{2\text{high}} \\ 0 & \text{elsewhere} \end{cases} \tag{4}$$

E. Feature Extraction and Classification Stage

Feature extraction is applied to represent the characteristics of the ROI. The features are measured directly from the ROI close regions, which are the mode, standard deviation, mean, median, and mean of the boundary. The features measured are shown in Fig. 8. These figures show two-dimensional (2-D) plots of the basic statistical characterization of ROI. Acute stroke and solid tumor are represented by blue and green, respectively. Necrosis and chronic stroke are represented by red and cyan, respectively. The plots show obvious distinction in cluster between hyper- and hypo-intensity lesions. In addition, the standard deviation can be used to separate acute stroke and solid tumor, while the mean boundary can be used to separate necrosis and chronic stroke.

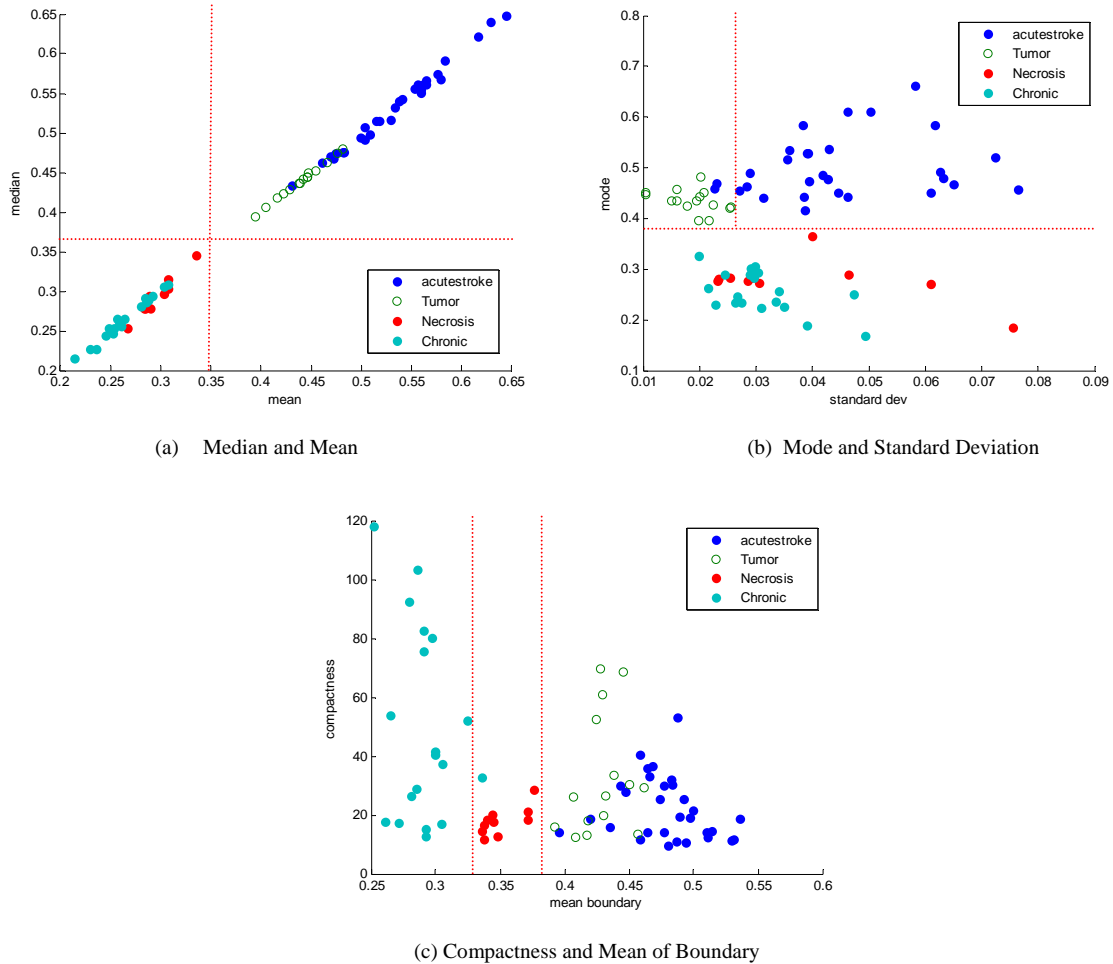


Fig. 8. ROI Features Distributions

For the classification process, a rule-based classifier is used [17, 18]. This is due to its simplicity as well as its ability to do multi-classification from various input features. The combinations of these features can differentiate the described lesions. The overall process of lesion classification is shown in the flowchart in Fig. 9.

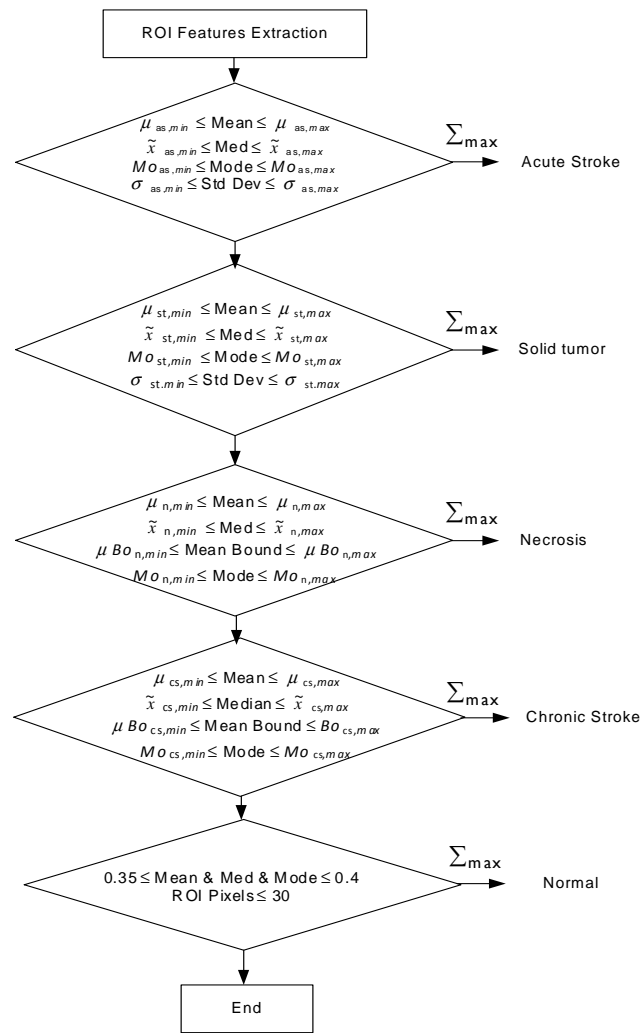


Fig. 9. Rule-Based Classification Process

F. Performance Evaluation

The segmentation results obtained from the proposed method are compared with the manual reference segmentation images, drawn by neuro-radiologists. In this analysis, area overlap (AO) based on Jaccard’s index is used to measure the accuracy of the segmentation for the pair of segmented and reference images [13]. The range is from 0 (no overlap) to 1 (complete congruence). However, the Jaccard’s overlap ratio is insensitive to over- or under-segmentation estimations. Therefore, false positive rate (FPR, over-segmentation error) and false negative rate (FNR, under-segmentation error) are also calculated to evaluate the error measures, using the following metrics:

$$AO = \frac{A \cap G}{A \cup G} \tag{5}$$

$$FPR = \frac{A \cap G^c}{A \cup G} \tag{6}$$

$$FNR = \frac{A^c \cap G}{A \cup G} \tag{7}$$

where A represents the segmentation results obtained by the proposed algorithm and G represents manual reference segmentation. AO computes Jaccard’s overlap ration between the segmentation and the manual reference. FPR and FNR are used to quantify over- and under-segmentation respectively. High AO, and low FPR and FNR show high accuracy and low error of the measurement. Accuracy of the correct classification is evaluated using Equation (8).

$$Accuracy = \frac{\sum \text{correct classification}}{\sum \text{number of samples}} \times 100 \quad (8)$$

III. RESULTS AND DISCUSSIONS

A. Brain Lesion Classification

For this study, 30 acute stroke, 15 solid tumor, 20 chronic stroke, and 10 necrosis cases have been used. The graphical user interface (GUI) for the system is developed for brain lesion classification. The view of the sample image in the GUI is given in Fig. 10.

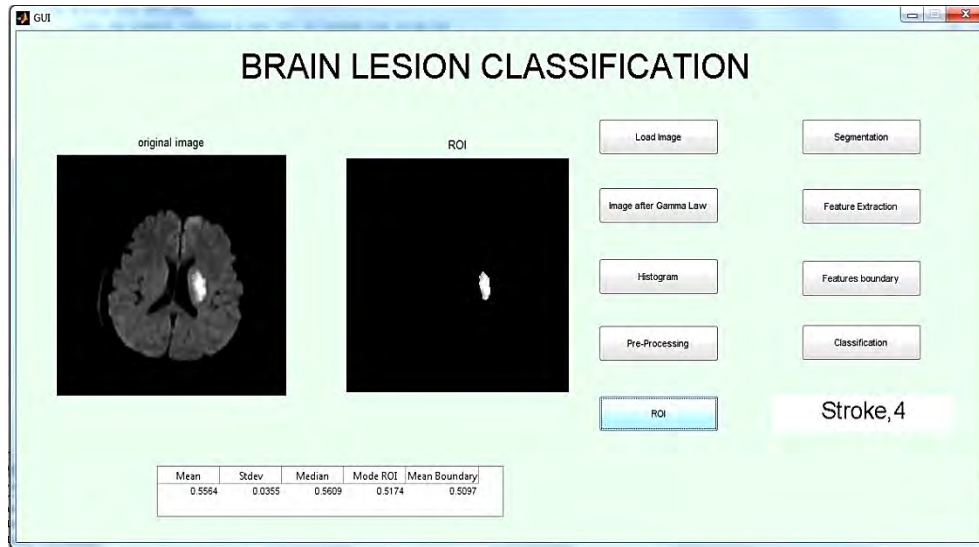


Fig. 10. Rule-Based Classification Process

B. Segmentation Performance and Error Rates

The proposed algorithm is tested on several DWI with various types of lesions. The hyper- and hypo-intensity lesions and their segmentation results are shown in Figs. 11 and 12. The arrows show the lesion's area in the original image. The DWI with acute stroke is shown in Fig. 11 (a), while Fig. 11 (b) shows a solid tumor lesion and its segmentation images.

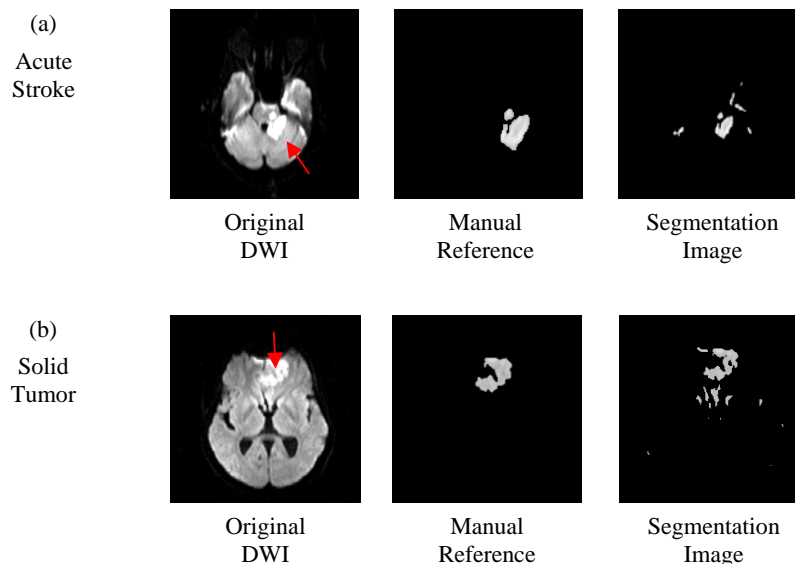


Fig. 11. Hyper-intensity Lesions Using Adaptive Thresholding and Manual Reference Image

Fig. 12 shows the hypo-intensity lesions for necrosis and chronic stroke. The results show that adaptive thresholding can successfully segment the hypo-intense lesion but fails to locate the area of the lesion. The cerebral spinal fluid (CSF) is located in the middle of the brain. It shares a similar intensity range with lesions

and is segmented as the lesion's region. This effect results in low overlap ratio performance for the adaptive thresholding method.

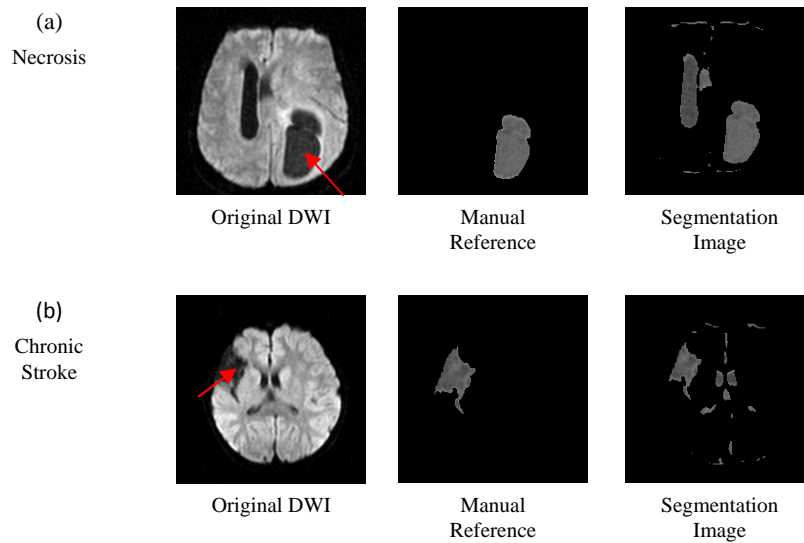


Fig. 12. Hypo-intensity Lesions Using Adaptive Thresholding and Manual Reference Image

Performances of the adaptive thresholding segmentation technique are shown in Table I. The results are based on 10 sample images for each of the cases. Each manual segmentation image needs to be handled by experts to perform the manual reference. The results show that for a hyper-intensity lesion, the overlap ratio is above 0.5, which is 0.8 for acute stroke, and 0.55 for solid tumor. The *FPR* and *FNR* errors are low, which are 0.14 and 0.06 for acute stroke and 0.3 and 0.15 for solid tumor, respectively. Solid tumor shows lower segmentation results compared to acute stroke. This is because the lesion region is irregular and partially blurry. In comparison with acute stroke, the lesion is high intensity and has clear boundaries.

Adaptive thresholding technique gives the worst result for all evaluations for chronic stroke and necrosis. This is due to the inability of the method to characterize the intensity between the lesions and CSF. CSF shares similar hypo-intensity and is located in the middle of the brain. It is symmetric and the area is big, thus resulting in over-segmentation error. The Jaccard's overlap ratio for chronic stroke is 0.27, while necrosis is 0.42. *FPR* are 0.72 (chronic stroke) and 0.43 (necrosis). For *FNR*, chronic stroke is 0.09 while necrosis is 0.15. The average segmentation performances are 0.512 (Jaccard's overlap ratio); 0.399 (false positive rate); and 0.112 (false negative rate). Adaptive thresholding segmentation provides the highest performance for acute stroke. However, performance for chronic stroke and necrosis is low. Overall, Jaccard's similarity index of the segmentation results for acute stroke, solid tumor, chronic stroke, and necrosis are 0.8, 0.55, 0.27, and 0.42, respectively.

TABLE I
Segmentation Evaluation Results

Lesions	Performance Index		
	Jaccard's Overlap Ratio (Area Overlap)	False Positive (FPR-Over Segmentation Error)	False Negative (FNR-Under Segmentation Error)
Acute Stroke	0.799	0.142	0.059
Solid Tumor	0.553	0.301	0.147
Chronic Stroke	0.272	0.635	0.093
Necrosis	0.424	0.43	0.146
Average	0.512	0.377	0.111

C. Classification Performance and Accuracy

The confusion matrix for the classification results is shown in Table II. This experiment is performed by training the classifier by 30% of samples, using a simple static split of data. The rest of the samples (75 images) are used for testing the classifier. The best classification performance is obtained for acute stroke that is composed of hyper-intensity features. The worst classification result is obtained for chronic stroke, because of its overlapping intensity with necrosis and CSF (normal-dark region). Average classification rate is achieved for

tumor, attributed to the fact that this lesion has similar characteristics to acute stroke and normal (iso-intense). Correct classifications are achieved at 0.9, 0.8, 0.63 and 0.8 for acute stroke, solid tumor, chronic stroke and necrosis, respectively.

TABLE II
Results of Confusion Matrix using 30% Static Split Data

Predicted	Actual					Correct Classification
	Acute Stroke	Solid Tumor	Chronic Stroke	Necrosis	Normal	
Acute Stroke	0.9	0.1				0.9
Solid Tumor	0.16	0.73			0.13	0.73
Chronic Stroke			0.63	0.37		0.63
Necrosis			0.1	0.8	0.1	0.8
Normal						1

The classification rate for the automatic system is shown in Fig. 13. The percentage of correct classification is 93% for acute stroke, 73% for solid tumor, 84% for chronic stroke, and 60% for necrosis. It is observed that the automated classification accuracy for hyper-intense lesions is comparable to the manual reference. Due to the overlap intensity on CSF and hypo-intense lesions, the classification accuracy for necrosis and chronic strokes are less sensitive. Overall, adaptive thresholding provides high segmentation performance for hyper-intensity lesions. The best segmentation and classification performance is achieved for acute stroke. Four types of lesions in DWI can be characterized by using a rule-based classification approach.

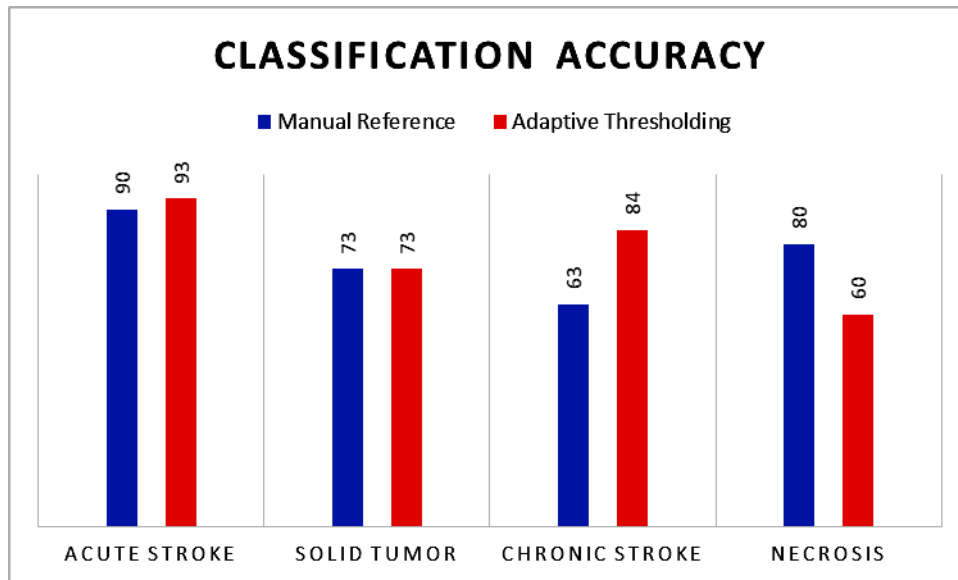


Fig. 13. Classification Accuracy for Manual and Adaptive Thresholding Segmentation

IV. CONCLUSION

A new DWI image analysis technique for segmentation and classification of brain lesions is demonstrated in this paper. Adaptive thresholding and a rule-based classifier are the method of choice to develop an automated brain classification system. Performance of the segmentation technique is evaluated and discussed. The graphical user interface (GUI) is developed to show the system database and technique for classification. Jaccard's similarity index of the segmentation results is 0.8, 0.55, 0.27, and 0.42, while the classification accuracy is 93%, 73%, 84%, and 60% for acute stroke, solid tumor, chronic stroke, and necrosis, respectively. The best segmentation and classification performance is achieved for acute stroke. Hypo-intense lesions and cerebral spinal fluid (CSF) share similar intensity, thus resulting in low segmentation and classification performance for necrosis and chronic stroke. The establishment of the technique could be used to automate the diagnosis and to clearly understand major brain lesions.

APPENDIX

Tables III and IV show some samples used for segmentation of hyper-intense (acute stroke and solid tumor) and hypo-intense lesions (chronic stroke and necrosis).

TABLE III
RESULTS OF HYPER-INTENSE LESIONS

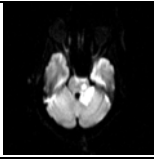
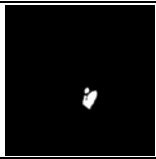

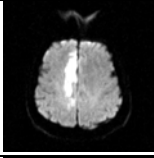
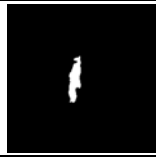
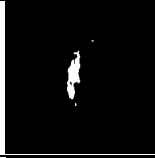
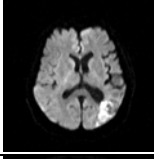
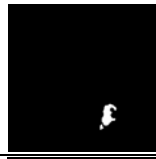
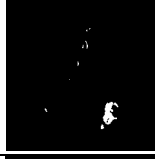
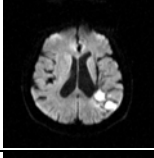
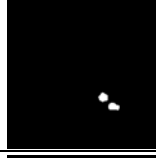
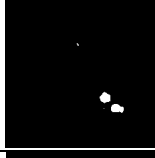
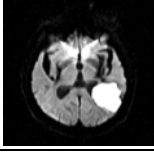
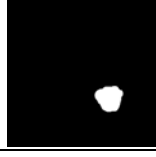

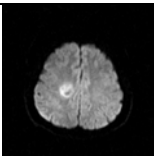
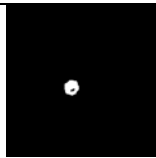

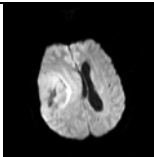

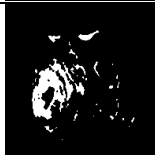
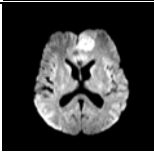

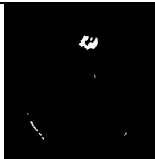
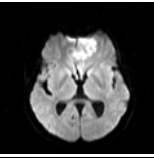
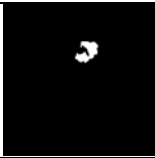

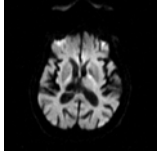


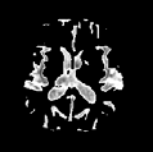
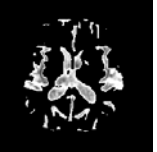
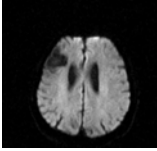




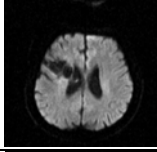




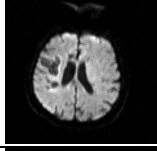
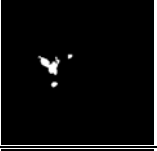
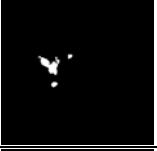


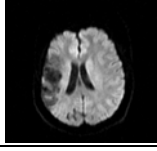
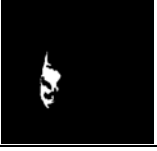
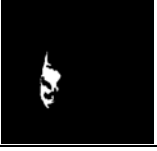


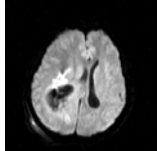
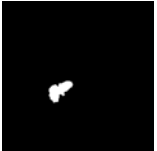
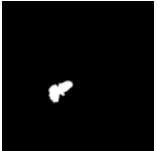


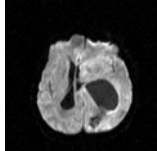
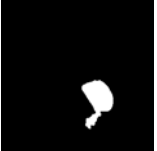
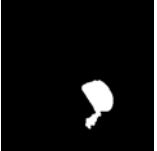


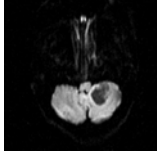
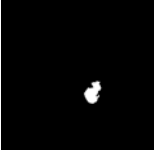
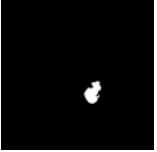


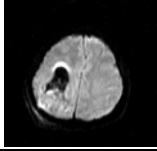
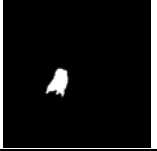
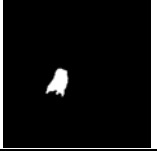


Original Image	Manual Reference	Adaptive Thresholding
Acute Stroke		
		
		
		
		
		
Solid Tumor		
		
		
		
		

TABLE IV
Results of Hypo-intense Lesions

Original Image	Manual Reference		Adaptive Thresholding	
Chronic Stroke				
				
				
				
				
				
Necrosis				
				
				
				
				

ACKNOWLEDGMENT

This work was supported by Universiti Teknikal Malaysia Melaka (UTeM) under Research University Grant S01142 - PJP/2013/FKEKK(4B) in collaboration with Universiti Teknologi Malaysia (UTM), and Universiti Kebangsaan Malaysia Medical Centre (UKMMC).

REFERENCES

- [1] S. J. Holdsworth, K. W. Yeom, M. U. Antonucci, J. B. Andre, et al. "Diffusion-Weighted Imaging with Dual-Echo Echo-Planar Imaging for Better Sensitivity to Acute Stroke." *American Journal of Neuroradiology* (2014).
- [2] Mukherji, Suresh K., Thomas L. Chenevert, and Mauricio Castillo. "Diffusion-Weighted Magnetic Resonance Imaging." *Journal of Neuro-Ophthalmology* 22, no. 2 (2002): 118-122.
- [3] MAGNETOM Maestro Class, "Diffusion Weighted MRI of the Brain," Siemens Medical Solutions that Help, 2010.
- [4] American Cancer Society: Cancer Facts and Figures 2014. (Atlanta, GA: American Cancer Society, 2014).
- [5] Health Facts 2012 – Ministry of Health Malaysia, July 2012.
- [6] K. Doi, "Computer-Aided Diagnosis in Medical Imaging: Historical Review, Current Status and Future Potential." *Computerized Medical Imaging and Graphics*, vol. 31, pp. 198–211, 2007.
- [7] J. Ruiz-Alzola, et al., "Editorial Advanced Signal Processing Methods for Biomedical Imaging." *International Journal of Biomedical Imaging*, Vol. (2013): 1–2.
- [8] Y.C. Hum, K.W. Lai et al, "Review on Segmentation of Computer-Aided Skeletal Maturity Assessment." *Advances in Medical Diagnostic Technology, Lecture Notes in Bioengineering*, (2014), Springer.
- [9] J. Ringenberg, M. Deob, V. Devabhaktunia, O. Berenfeldc, P. Boyersd, J. Gold "Fast, Accurate, and Fully Automatic Segmentation of the Right Ventricle in Short-axis Cardiac MRI." *Computerized Medical Imaging and Graphics* 38 (2014): 190–201.
- [10] J. Jiang, Y. Wu, M. Huang, W. Yang, W. Chen, Q. Feng "3D Brain Tumor Segmentation in Multimodal MR Images based on Learning Population- and Patient-Specific Feature Sets." *Computerized Medical Imaging and Graphics* 37 (2013): 512–521.
- [11] P. R. Bai, Q. Y. Liu, L. Li, S. Hua Teng, J. Li, and M. Y. Cao "A Novel Region-based Level Set Method Initialized with Mean Shift Clustering for Automated Medical Image Segmentation." *Computers in Biology and Medicine* 43 (2013): 1827–1832.
- [12] Rafael C. Gonzales and Richard E. Woods. *Digital Image Processing*, 2nd Edition (2002).
- [13] N. Mohd Saad, S. A. R. Abu-Bakar, Sobri Muda, M. Mokji, and A. R. Abdullah, "Automated Region Growing for Segmentation of Brain Lesion in Diffusion-Weighted MRI." *Proceedings of the International MultiConference of Engineers and Computer Scientists*, 2012.
- [14] D-M Koh and A. R. Padhani, "Diffusion-Weighted MRI a New Functional Clinical Technique for Tumour Imaging." *The British Journal of Radiology* 79, no 944 (January 2014).
- [15] N. M. Saad, S. A. R. Abu-Bakar, Sobri Muda, M. Mokji, "Segmentation of Brain Lesions in Diffusion-Weighted MRI Using Thresholding Technique." *Proceedings of the 2011 International Conference on Signal and Image Processing Applications (ICSIPA)*, 2011, pp 249-254.
- [16] N. Otsu, "A Threshold Selection Method from Gray-Level Histogram." *IEEE Transaction on System Man Cybernetics* 9, no. I (1979): 62–66.
- [17] O. R. Zaiane, M.-L. Antonie, and A. Coman, "Mammography Classification by an Association Rule-Based Classifier." *Proc. MDK/KDD 2002: International Workshop Multimedia Data Mining*, 62–69 (2002).
- [18] R.O. Duda, P.E.Hart, and D.G. Stork, *Pattern Classification*, 2nd Edition (2001).